The Dependence of Star Formation History and Internal Structure on Stellar Mass for 80,000 Low-Redshift Galaxies

Guinevere Kauffmann[1], Timothy M. Heckman[2], Simon D.M. White[1], Stéphane Charlot[1,3], Christy Tremonti[2], Eric W. Peng[2], Mark Seibert[2], Jon Brinkmann[4], Robert C. Nichol[5], Mark SubbaRao[6]

[1] *Max-Planck Institut für Astrophysik, D-85748 Garching, Germany*

[2] *Department of Physics and Astronomy, Johns Hopkins University, Baltimore, MD 21218*

[3] *Institut d'Astrophysique du CNRS, 98 bis Boulevard Arago, F-75014 Paris, France*

[4] *Apache Point Observatory, P.O. Box 59, Sunspot, NM 88349*

[5] *Department of Physics, Carnegie Mellon University, 5000 Forbes Ave, Pittsburgh, PA 15232*

[6] *Department of Astronomy, University of Chicago, 5640 South Ellis Ave, Chicago, IL 60637*

Abstract

We study the relations between stellar mass, star formation history, size and internal structure for a complete sample of 80,000 galaxies drawn from the Sloan Digital Sky Survey. We show that low-redshift galaxies divide into two distinct families at a stellar mass of $3 \times 10^{10} M_\odot$. Lower mass galaxies have young stellar populations, star formation histories characterized by recent bursts, low surface mass densities, and the low concentrations typical of disks. At given stellar mass their sizes are log-normally distributed with dispersion $\sigma(\ln R_{50}) \sim 0.5$, in excellent agreement with the idea that they form with little angular momentum loss through cooling and condensation in a gravitationally dominant dark matter halo (Fall & Efstathiou 1980). Their median stellar surface mass density scales with stellar mass as $\mu_* \propto M_*^{0.6}$, suggesting that the stellar mass of a disk galaxy is proportional to the five thirds power of its halo mass. The galaxies with the lowest stellar surface densities most frequently exhibit the spectral signature of a recent starburst. All this points to a picture in which the star formation efficiency increases in proportion to halo mass, perhaps as a result of supernova feedback processes. At stellar masses above $3 \times 10^{10} M_\odot$, there is a rapidly increasing fraction of galaxies with old stellar populations, high surface mass densities and the high concentrations typical of bulges. In this regime, the size distribution remains log-normal, but its dispersion decreases rapidly with increasing stellar mass and the median mass surface density increases more slowly ($\propto M_*^{0.2}$). This suggests that the star formation efficiency has saturated, and that little star formation occurs in massive galaxies after they have assembled.

1 Introduction

Perhaps the most remarkable aspect of galaxies is their regularity – the fact that they can be classified into well-defined sequences. Hubble (1926) introduced the first scheme to categorize galaxies according to morphological type, and its basic concepts are still in use today. In its simplest form, three basic galaxy types are recognized: ellipticals, spirals and irregulars. These can be arranged in a linear sequence along which many properties vary coherently. The most striking trends are the variations in morphology (featureless ellipsoid to spiral disk to irregular appearance) and in colour and star formation activity. These trends were so striking that they formed the basis of Hubble's original scheme. Elliptical galaxies have red colours, little gas and no ongoing star formation; irregulars have blue colours, large gas fractions and are actively forming stars. An up-to-date review of star formation along the Hubble sequence is given in Kennicutt (1998a).

It should be remembered that Hubble introduced his galaxy classification scheme at a time when distance estimates were available for only a handful of galaxies. Hubble could not study the properties of galaxies as a function of parameters that measure their *absolute scale*: sizes, absolute magnitudes and masses. Today it is known that the distribution of Hubble types depends strongly on galaxy luminosity. The typical elliptical galaxy is a factor ~ 10 more luminous in the B-band than the typical irregular galaxy (Roberts & Haynes 1994). As a result, the faint end of the galaxy luminosity function is dominated by late-type galaxies with strong emission lines and the bright end by early-type galaxies with little star-formation (e.g. Loveday et al 1992; Marzke et al 1994; Lin et al 1996; Zucca et al 1997; Marzke et al 1998; Christlein 2000). These trends in star formation activity become even more pronounced when studied in the near-infrared. This has led to suggestions that the ratio of present to past-averaged star formation rate may depend primarily on stellar mass and only secondarily on morphological type (Boselli et al 2001; Balogh et al 2001).

There have been many studies of stellar populations and star formation histories that focus on galaxies of a particular Hubble type. The star formation rates in most irregular and dwarf galaxies in the Local Group do not appear to have varied smoothly with time, but instead have undergone large fluctuations or "bursts" (see Grebel 2000 for a recent review). There is evidence that the recent star formation histories of spirals depend on the surface brightness of their disks. Low surface brightness galaxies appear to have bluer colours and higher gas mass fractions than high surface brightness galaxies (de Blok, van der Hulst & Bothun 1995; de Blok, McGaugh & van der Hulst 1996). The situation for ellipticals is currently unclear. Although there is considerable evidence that the absorption line strengths of early-type galaxies vary systematically with their velocity dispersions, there is much debate as to whether this reflects trends in stellar age, in metallicity or in the relative abundance of different heavy elements (e.g. Trager et al 1998; Kuntschner et al 2001).

The Sloan Digital Sky Survey will obtain u, g, r, i, and z-band photometry, spectra and redshifts for at least 700,000 galaxies down to a limiting r-band magnitude of 17.77. This is the most ambitious survey of the local galaxy population ever undertaken and motivates a critical re-evaluation of trends in the star formation histories of galaxies as a function of mass, size, internal structure and environment.

We have recently developed a new method to constrain the star formation history, and to estimate the dust attenuation and stellar mass of galaxies (Kauffmann et al 2002; hereafter Paper I). It is based on two stellar absorption line indices, the 4000 Å break strength and the Balmer absorption line index Hδ_A. These indices allow us to constrain the mean stellar age of a galaxy and the fraction of its stellar mass formed in bursts over the past few Gyr. A comparison with broad band photometry then yields estimates of dust attenuation and of stellar mass. We have generated a large library of Monte Carlo realizations of different star formation histories, including starbursts of varying strength. We have used this library to generate likelihood distributions for parameters such as burst mass fraction, dust attenuation strength, stellar mass and stellar mass-to-light ratio for every galaxy in a complete sample of 80,000 objects drawn from the Sloan Digital Sky Survey.

Paper I introduced our method and used it to measure how the total stellar mass of the Universe is distributed over galaxies as a function of their stellar mass, size, concentration, colour and surface mass density. In this paper, we focus on the *mass dependence* of the star formation histories, sizes and structural parameters of galaxies. We study to what extent the recent star formation histories of galaxies of different stellar mass can be characterized as continuous or as burst-dominated. We also show how the distributions of structural parameters (size, surface mass density, concentration index) vary with stellar mass, and we demonstrate that variations in star formation history and in structural parameters are tightly coupled. Finally, we interpret our findings in the context of current theories of galaxy formation.

2 Review of the Observed and Derived Parameters of Galaxies

The sample of galaxies analyzed in this paper is drawn from the Sloan Digital Sky Survey (York et al 2000; Stoughton et al 2002). We have included all galaxies with spectroscopic observations taken prior to MJD 52078 and with Petrosian r band magnitudes in the range $15.5 < r^* < 17.7$ after correction for foreground galactic extinction. Details about the spectroscopic target selection may be found in Strauss et al (2002). These data represent roughly 10% of the projected survey total and include a total of 81,429 galaxies.

The reader is referred to Paper I for more information about the sample and a detailed description of the methods used to derive parameters such as stellar mass and burst mass fraction. Here we provide a brief summary of the quantities that are studied in this paper:

1. **Absolute magnitudes:** All magnitudes quoted in this paper are Petrosian magnitudes. In order to convert from apparent to absolute magnitude, we assume a Friedman-Robertson-Walker cosmology with $\Omega = 0.3$, $\Lambda = 0.7$ and H_0= 70 km s $^{-1}$ Mpc^{-1}. We have used the most recent version of the Bruzual & Charlot (1993) models to generate

lookup tables of K-corrections to the rest-frame magnitudes of galaxies based on their observed colours and on redshift. More details about the SDSS photometric system may be found in Fukugita et al (1996) and Smith et al (2002). Information relating to the SDSS camera and photometric monitoring system can be found in Gunn et al (1998) and Hogg et al (2001). A technical paper describing the astrometry in the survey has recently been published by Pier et al (2002).

2. **Stellar spectral indices:** We have adopted the narrow definition of the 4000 Å break introduced by Balogh et al (1999), which we denote $D_n(4000)$. We also use the Balmer absorption index $H\delta_A$ as defined by Worthey & Ottaviani (1997) using a central bandpass bracketed by two continuum bandpasses. As discussed in Paper I, the $D_n(4000)$ index is an excellent age indicator for young ($< 1-2$ Gyr, $D_n(4000) < 1.5$) stellar populations, but for older stellar populations, the index depends quite strongly on metallicity. Strong Balmer absorption occurs in galaxies that experienced a burst of star formation 0.1-1 Gyr ago. Analyzed together, the two indices are a powerful probe of the recent star formation history of a galaxy. Because each is defined over a narrow wavelength interval, they are not sensitive to dust attenuation effects.

3. **Stellar masses:** The stellar masses are derived assuming a universal initial mass function (IMF) in the parametrisation of Kroupa (2001). Other choices of IMF can change the overall normalization (for example, a Salpeter IMF truncated at $0.1 M_\odot$ gives stellar masses a factor of two larger than the Kroupa IMF). We note, however, that our choice of IMF does not affect our conclusions about the scaling of galaxy properties as a function of mass. It predicts stellar masses for massive galaxies which are consistent with their dynamically estimated masses (see Paper I).

4. **Burst mass fractions:** We define the parameter F_{burst} as the fraction of the total stellar mass of a galaxy that formed in "burst" mode over the past 2 Gyr. In Paper I we showed that galaxies with continuous star formation histories occupy a very narrow locus in the $H\delta_A/D_n(4000)$ plane. Galaxies that experienced recent bursts have $H\delta_A$ values that are displaced from this locus.

5. **Galaxy sizes:** We study the distribution functions of $R50(z)$, the radius enclosing 50% of the Petrosian z-band luminosity of a galaxy. We note that the sizes output by the current SDSS photometric pipeline have not been corrected for seeing effects (Stoughton et al 2001).

6. **Concentration indices:** In order to be consistent with previous work (Blanton et al 2001; Strateva et al 2001; Shimasaku et al 2001) we define the concentration index C as the ratio $R90/R50$, where R90 and R50 are the radii enclosing 90% and 50% of the Petrosian r-band luminosity of the galaxy.

7. **Surface brightnesses and surface mass densities:** Following Blanton et al (2001), we define the half-light surface brightness $\mu_{1/2}$ to be the average r-band surface brightness within the r-band half-light radius R50 in magnitudes per square arcsecond. The main spectroscopic survey is complete down to a limiting half-light surface brightness $\mu_{1/2} = 24.5$ mag arcsec^{-2}. We define the surface mass density μ_* as $0.5M_*/[\pi R50^2(z)]$, where $R50(z)$ is the Petrosian half-light radius in the z-band (we choose a radius defined in the z-band rather than r-band, as this provides a better approximation to the radius enclosing half the total stellar mass).

In this paper, we will often use bivariate density distributions $\phi(x, y)$ in the parameters x and y, defined such that $\phi(x, y)dx\, dy$ is the number of galaxies per unit volume with x in the interval $(x, x+dx)$ and y in the interval $(y, y+dy)$. Such bivariate distributions are calculated by weighting each galaxy in the sample by $1/V_{max}$, where V_{max} is the volume corresponding to the total redshift range over which the galaxy would pass the survey selection criteria. In many cases we will be interested in trends in the distribution of the parameter y as a function of the parameter x (for example in the distribution of concentration or size as a function of stellar mass). In such cases, we make the trends more visible by plotting the conditional distribution of y given x, i.e. $\phi(x, y)/\int \phi(x, y')dy'$.

3 The Observed Correlations

3.1 The Dependence of Star Formation History on Stellar Mass

In Fig. 1, we present the conditional density distributions of our two stellar age indicators $D_n(4000)$ and $H\delta_A$ as a function of stellar mass and as a function of g-band absolute magnitude. The grey-scale indicates the fraction of galaxies in a given logarithmic mass (or magnitude) bin that fall into each age-indicator bin. The contours are separated by factors of 2 in population density.

It is clear that $D_n(4000)$ and $H\delta_A$ depend strongly both on stellar mass and on absolute magnitude. The main effect of transforming from luminosity to mass is to produce a more regular variation of the indices. Fig. 1 shows that low mass galaxies are typically young. At a mass of $M_* \sim 3 \times 10^{10}$ $M_\odot$, a transition towards older stellar populations begins to take effect. Almost all of the most massive galaxies in our sample have old stellar populations. We note that high mass galaxies occupy a narrow range in $D_n(4000)$ and $H\delta_A$. Low mass galaxies, on the other hand, occupy a narrow range in $D_n(4000)$, but a wide range in $H\delta_A$. As we will discuss below, this is the signature of a population whose recent star formation history is punctuated by bursts.

Fig. 2 shows "slices" through the $D_n(4000)$-M_* distribution. Note that the measurement error on the $D_n(4000)$ index is very small, typically around 0.02, or a few percent of the total range of values spanned by galaxies in our sample. Again, one sees a striking trend towards older stellar populations for galaxies with larger stellar masses. Both in Fig. 1 and in this plots one gets the impression of two separate and relatively well-defined populations whose relative weight changes systematically and smoothly with stellar mass. It is interesting that in our lowest mass bin, there is a small but significant increase in the fraction of galaxies with large 4000 Å break strengths. In the Local Group, there is a known population of dwarf elliptical (dE) galaxies with old stellar populations and no ongoing star formation. Such objects are apparently rare at stellar masses greater than $10^8 M_\odot$.

The bivariate density distribution of Hδ_A and D$_n$(4000) is shown in Fig. 3 for galaxies in 8 ranges of stellar mass spanning four orders of magnitude from $M_* = 10^8 M_\odot$ to $M_* = 10^{12} M_\odot$. In these plots, the grey scale indicates the fraction of galaxies that fall into each bin of $H\delta_A$ and D$_n$(4000). It is striking how galaxies move diagonally across the Hδ_A/D$_n$(4000) plane as their masses increase. One can see clearly that low mass galaxies with $D_n(4000) < 1.5$ (characteristic of stellar populations with mean ages of less than a few Gyr) have a larger scatter in Hδ_A equivalent width than high mass galaxies with similar break strengths. This means that the fraction of low mass galaxies that have experienced recent bursts is high and the fraction of high mass galaxies with recent bursts is low, even when the two populations are compared at similar mean stellar age.

In Paper I, we introduced models in which galaxies formed stars in two different modes: i) a "continuous" mode , which we parametrized by an exponential law with timescale τ and starting time t_{form}, and ii) a superposed "burst" mode. A burst was defined to be an episode of star formation lasting between 3×10^7 and 3×10^8 years in which a fraction F_{burst} of the total stellar mass of the galaxy was formed. In Paper I, we introduced a method that allowed us to calculate the *a posteriori* likelihood distribution of F_{burst} for each galaxy in our sample, given its observed absorption line indices. In Fig. 4, we plot the distribution of galaxies as a function of F_{burst} for the same set of 8 mass ranges. For this plot we take the "best" estimate of F_{burst} to be the median value of the likelihood distribution. From now on we will denote this quantity as $\bar{F}_{burst}$. The distribution of galaxies over $\bar{F}_{burst}$ is shown as a solid histogram in Fig. 4. The dashed histogram shows the distribution of galaxies as a function of the lower 2.5 percentile value of F_{burst}. We note that the widths of the likelihood distributions of F_{burst} are quite broad for most galaxies in our sample. The typical 1σ error on F$_{burst}$ is around 0.15. It is only for the most extreme galaxies with $\bar{F}_{burst} > 0.5 - 0.6$ that we can determine burst mass fractions to better than 25% using our method.

In our lowest mass range ($10^8 - 3 \times 10^8 M_\odot$), we find that 45% of all galaxies are *likely* to have undergone a burst in the past 2 Gyr. However, it is only for 10% of these objects that we can state with high (>97.5%) confidence that a burst *did occur* in the recent past. The fraction of galaxies that have experienced recent bursts decreases very strongly with increasing stellar mass. Less than 2% of galaxies with masses comparable to our own Milky Way are likely to have experienced a burst of star formation in the past 2 Gyr. We also find that the most likely values of the burst mass fractions correlate with stellar mass. The starbursts that do occur in high mass galaxies appear to involve a smaller fraction of the total mass. This is not surprising; it is well known that more massive galaxies have lower gas mass fractions and thus contain less fuel for star formation (e.g. Roberts & Haynes 1994; Boselli et al 2001; Bell

& de Jong 2001).

We now study how the probability of a recent starburst depends on the luminosity-weighted stellar age of the galaxy. In Fig. 5, we plot histograms of the fraction of galaxies with $\bar{F}_{burst} > 0$ as a function of the index $D_n(4000)$ for different ranges in stellar mass. Recall that $D_n(4000)$ is a reasonably good proxy for stellar age at index values below ~ 1.5. At higher values, $D_n(4000)$ depends both on age and on metallicity, so the interpretation of the observed trends is more complicated. Because most low-mass galaxies have small break strengths and most high-mass galaxies have large break strengths, the number of galaxies falling into each bin in $D_n(4000)$ is not constant. We have included error bars to indicate the $\pm 1\sigma$ uncertainty in each bin.

From Fig. 5 we see that virtually all galaxies with $D_n(4000) < 1.1$ have $\bar{F}_{burst} > 0$. These galaxies are simply too young to be consistent with any of our continuous star formation models. (Recall from Paper I that the youngest galaxy in our library begins forming stars 1.5 Gyr in the past.) Many of these galaxies are probably experiencing a starburst at the present day. We also see that the fraction of galaxies with $\bar{F}_{burst} > 0$ decreases as a function of $D_n(4000)$ in all mass bins except the lowest one. Note that there is a "dip" in all the histograms at $D_n(4000)$=1.2. This feature is another consequence of our requiring all galaxies to begin forming stars at least 1.5 Gyr ago. For galaxies with $D_n(4000)$ values in the range $1.2 - 1.5$, the fraction of galaxies with $\bar{F}_{burst} > 0$ is much larger for low mass galaxies than for high mass galaxies. The statistical significance of this trend is extremely high. The fact that low mass galaxies are more likely to have had a recent starburst (Fig. 4) is thus *not* a simple consequence of their being younger than high mass galaxies. Fig. 5 demonstrates that the mode of star formation differs between low mass and high mass galaxies of similar mean stellar ages.

Finally, in Fig. 6 we compare the distributions of Hα emission line equivalent widths for galaxies with $\bar{F}_{burst} > 0$ and $\bar{F}_{burst} = 0$. We have divided the sample into different bins in $D_n(4000)$ in order to take into account any systematic mean age difference between galaxies with and without recent bursts. As can be seen, there is a tendency for galaxies that have experienced a recent starburst to have slightly *stronger* Hα emission than other galaxies of similar age. Recent starbursts clearly do not truncate subsequent ongoing star formation in the majority of galaxies.

3.2 The Dependence of Structural Parameters on Stellar Mass

In Fig. 7, we present conditional density distributions for concentration index C, r-band half-light surface brightness $\mu_{1/2}$, and surface mass density μ_* as functions of stellar mass and of r-band absolute magnitude. Fig. 7 demonstrates that the structural parameters of galaxies correlate both with absolute magnitude and with stellar mass, but once again we find that the trends are tighter when plotted as a function of stellar mass.

The surface mass density exhibits a strikingly tight correlation with stellar mass. μ_* increases by nearly two orders of magnitude from $\sim 10^7 M_\odot$ kpc^{-2} for galaxies with $M_* \sim$

$10^8 M_\odot$ to $\sim 10^9 M_\odot$ kpc^{-2} for the most massive galaxies with $M_* = 10^{12} M_\odot$. In contrast, the r-band surface brightness only increases by a factor of 4 as $M(r)$ increases by 8 magnitudes. There is a sharp change in slope in the $\mu_* - M_*$ relation at a stellar mass of $\sim 3 \times 10^{10} M_\odot$. A transition at the same stellar mass is also seen in the $C - M_*$ relation. Interestingly, this is also the stellar mass at which galaxies switch from young to old in Fig. 1. It is important to note that virtually all galaxies in our sample with $M_* > 10^8 M_\odot$ have $\mu_{1/2} < 23.5$ mag arcsec^{-2}. The main spectroscopic survey is complete to surface brightnesses a magnitude fainter than this, so our results should not be biased by surface brightness selection effects.

Fig. 8 presents the size distributions for galaxies in eight disjoint ranges of stellar mass. We plot the fraction of galaxies as a function of the natural logarithm of the half-light radius in the z-band. These size distributions are extremely well described by a log-normal function

$$P(R)dR = \frac{1}{\sqrt{2\pi}\sigma} \exp\left[-\frac{(\ln(R/R_{med}))^2}{2\sigma^2}\right] \frac{dR}{R}, \tag{1}$$

where R_{med} is the median value of the size distribution and σ is the dispersion in $\ln R$. We have indicated the value of σ and R_{med} for the lognormal fit in each panel in Fig. 8. The *shape* of the size distribution is independent of mass for galaxies with $M_* < 3 \times 10^{10} M_\odot$ and is well fit by $\sigma \sim 0.5$. The median size R_{med} scales with stellar mass as $R_{med} \propto M_*^{0.15}$. For stellar masses larger than $3 \times 10^{10} M_\odot$, the shape of the size distribution is still lognormal, but the dispersion decreases. R_{med} also increases more rapidly with mass ($\propto M_*^{0.3}$) in this regime.

Figs. 9 and 10 show the distributions of concentration index C and surface mass density μ_* for these same eight stellar mass ranges. The distribution of C is nearly independent of stellar mass for galaxies with $M_* < 3 \times 10^{10} M_\odot$. The median value of C for these systems is around 2.3. Only about 10% of low mass galaxies have $C > 2.6$, the value that marks the transition from late-type to early-type morphologies (Strateva et al 2001). At larger masses, the distribution shifts to progressively higher concentrations. In our highest mass bin 90% of galaxies have C index values larger than 2.6. Fig. 10 shows that for galaxies with $M_* < 3 \times 10^{10} M_\odot$, the median surface mass density scales with stellar mass as $\mu_* \propto M_*^{0.7}$. The μ_* distribution is fairly broad and its shape does not appear to depend very strongly on stellar mass. At values of M_* larger than $3 \times 10^{10} M_\odot$, the scaling of of the median value of μ_* with stellar mass becomes much weaker ($\mu_* \propto M_*^{0.35}$). The shape of the distribution function skews and is eventually strongly peaked at values of μ_* around $10^9 M_\odot$ kpc^{-2}.

We note that all structural parameters discussed in this section have been calculated within circular apertures. We have estimated the additional scatter in size resulting from variations in inclination and find that this has very small effect on the values of the dispersion σ that we estimate.

3.3 The Connection Between Star Formation History and Structural Parameters

In the previous two subsections we showed that both the star formation histories and the structural parameters of galaxies depend strongly on stellar mass. It is therefore not surprising that the star formation histories of galaxies correlate with μ_* and C. This is illustrated in Fig. 11 where we present the conditional density distributions of the two stellar absorption indices $D_n(4000)$ and $H\delta_A$ as functions of surface mass density and of concentration. Galaxies with low surface density have young stellar populations and galaxies with high surface density have old stellar populations, with a strong transition at $\mu_* \sim 3 \times 10^8 M_\odot$ kpc^{-2}. There is also a striking transition in the values of $D_n(4000)$ and $H\delta_A$ at C values around 2.6. We note that this corresponds very well to the value of C recommended by Strateva et al (2001) for optimum separation between early and late Hubble types, based on an analysis of a small sample of galaxies classified by eye.

We now ask whether it is possible to pinpoint the *primary* cause of variations in the star formation history of galaxies – do galaxies form stars in the burst mode because their masses are small or because their surface mass densities are low? We attempt to address this question in Figs. 12 and 13, where we plot the fraction of galaxies with $\bar{F}_{burst} > 0$ as a function of surface mass density at fixed stellar mass (Fig. 12), and as a function of stellar mass at fixed surface mass density (Fig.13). We have included errorbars on our histograms in order to show the uncertainty produced by the large variation in the number of galaxies in each bin. Figures 12 and 13 show that the fraction of galaxies that have experienced a recent starburst depends primarily on μ_*, rather than on stellar mass. In fact, Fig. 12 indicates that the relation between burst fraction and μ_* *depends at most weakly on stellar mass*. Similar trends are also found for the $D_n(4000)$ index.

3.4 Summary

In the previous subsections, we demonstrated that there are strong correlations between the star formation histories, stellar masses and structural parameters of galaxies. Here we provide a summary of our results:

1. Low mass galaxies have young stellar populations. High mass galaxies have old stellar populations. A sharp transition from young to old occurs at a stellar mass of around $3 \times 10^{10} M_\odot$.

2. Low mass galaxies have low surface mass densities and low concentrations. High mass galaxies have high surface mass densities and high concentrations. An abrupt change in the slopes of the $\mu_* - M_*$ and $C - M_*$ relations occurs at a stellar mass of $3 \times 10^{10} M_\odot$.

3. The size distribution function of galaxies less massive than $3 \times 10^{10} M_\odot$ is well characterized by a lognormal distribution with dispersion $\sigma = 0.5$. Galaxies more massive than

$3 \times 10^{10} M_\odot$ also have a lognormal size distribution, but the dispersion decreases with increasing stellar mass.

4. Below the transition mass the median size of galaxies increases as $M_*^{0.15}$. Above the transition mass the increase is more rapid, $R \propto M_*^{0.3}$.

5. Galaxies with low surface mass densities and low concentrations have young stellar populations. Galaxies with high surface mass densities and high concentrations have old stellar populations. The transition from young to old stellar populations occurs at $\mu_* \sim 3 \times 10^8 M_\odot$ kpc^{-2} and $C \sim 2.6$.

6. The fraction of galaxies that have experienced recent starbursts decreases strongly with increasing stellar mass and with increasing surface mass density. We find, however, that at fixed surface mass density, the fraction of galaxies that have experienced recent starbursts is nearly independent of stellar mass.

7. Galaxies that have experienced recent starbursts have present-day star formation rates that are very similar to galaxies that have not had recent starbursts, if the comparison is made at a fixed value of D$_n$(4000).

4 Interpretation and Discussion

Our analysis has demonstrated that there is a sharp transition in the physical properties of galaxies at a stellar mass of $\sim 3 \times 10^{10} M_\odot$. Galaxies less massive than this have low surface mass densities, low concentration indices typical of disks, young stellar populations, and recent star formation histories characterized by bursts. More massive galaxies have high surface mass densities, high concentration indices typical of bulges, and predominantly old stellar populations.

An important clue to the physical process responsible for imprinting this characteristic mass scale comes from the recent discovery that the relation between stellar mass and gas-phase metallicity measured from emission line ratios shows a pronounced break at a stellar mass of $\sim 3 \times 10^{10} M_\odot$ (Tremonti et al 2002). At lower masses the metallicity of SDSS galaxies scales as $Z \propto M_*^{0.5}$; at higher masses, the metallicity saturates at values just above solar. As discussed by Tremonti et al, the most natural interpretation of this flattening is that $3 \times 10^{10} M_\odot$ represents the mass scale at which the efficiency of star formation approaches unity and so the metallicity approaches the yield. At lower masses feedback effects prevent conversion of a large fraction of protogalactic gas into stars and may eject a substantial fraction of it as a galactic wind. Such a transition should plausibly occur at the mass scale where the energy injected into the interstellar gas by supernovae is comparable to its binding energy within the galaxy. Multiphase models of the interstellar medium suggest that the star-formation process regulates itself in such a way that the hot space-filling gas is at a temperature of 10^6K or so, independent of the larger scale properties of the galaxy (McKee & Ostriker 1977; Efstathiou

2000). This temperature is close to the virial temperature expected in the halo of a present-day galaxy of stellar mass $3 \times 10^{10} M_\odot$, so it is plausible that feedback will reduce star formation efficiencies in lower mass systems but not in higher mass ones. Small systems will have low metallicities, large gas fractions, and may have lost much gas in a wind. High mass systems will retain their baryons turning most of them into stars. Their mean stellar metallicities will then be close to the time-averaged yield, which is indeed close to solar for a standard IMF. The high mass galaxies in the Tremonti et al. sample have *gas-phase* metallicities of $\sim 1.5 - 2$ times the solar value, consistent with the idea that they have retained most of their metals.

The results in this paper suggest that the process responsible for regulating the metallicity of galaxies may also play a major role in determining their structure and their star formation histories. As shown in Figures 7 and 9, the great majority of galaxies with stellar masses below $3 \times 10^{10} M_\odot$ have concentration indices below 2.6 and so are plausibly disk-dominated. At masses above $3 \times 10^{10} M_\odot$, the fraction of galaxies with $C > 2.6$ increases strongly. In our final mass bin ($M_* > 3 \times 10^{11} M_\odot$), 90% of the galaxies are bulge-dominated.

The size distribution of disk galaxies is of particular interest, because it can be compared directly to simple theoretical models. In a classic paper in 1980, Fall & Efstathiou considered the formation of a disk by the condensation of gas in a gravitationally dominant dark matter halo. If the gas initially has the same specific angular momentum as the dark matter and conserves its angular momentum during its contraction, then the characteristic radius of the disk will scale as

$$R_d \propto \lambda R_{halo}, \tag{2}$$

where R_{halo} is the virial radius of the halo. The spin parameter λ is defined as

$$\lambda = J|E|^{1/2} G^{-1} M^{-5/2}, \tag{3}$$

where E is the total energy of the halo, J is its total angular momentum and M is its total mass (see Mo, Mao & White (1998) for a detailed analytic model).

N-body simulations show that in hierarchical clustering cosmologies, the distribution of λ for dark matter halos has lognormal form with parameters which depend very weakly on cosmology or on halo mass (Barnes & Efstathiou 1987; Warren et al 1992; Cole & Lacey 1996; Lemson & Kauffmann 1999) with typical values $\lambda_{med} \simeq 0.04$ and $\sigma_\lambda \simeq 0.5 - 0.6$. The fact that for low mass galaxies the shape and width of the size distributions in Fig. 8 agree so well with this simple theory is truly remarkable.

It is not obvious how the stellar mass of a galaxy should scale with the mass of its dark matter halo. For simplicity, one might assume that a fixed fraction of the baryonic mass ends up in disk stars, in which case $M_* \propto R_{halo}^3$ and $R_d \propto M_*^{1/3}$ (this assumes that baryons follow the dark matter, at least initially). From Fig. 8, we find that median size increases *more slowly* than predicted by this simple model. This means that the stellar mass fraction must *increase* with halo mass. As noted above such an increase of star formation efficiency with halo mass is expected in a model where supernova feedback controls the dynamics of the interstellar medium. In most feedback models, supernovae inhibit the formation of stars in low mass halos, leading to small values of M_*/M_{halo} (e.g. White & Frenk 1991; Kauffmann, White & Guiderdoni 1993; Cole et al 1994). However, because we do not have any information about the gas fractions of the galaxies in our sample, we cannot say whether the suppression of star formation occurs because gas is expelled from the galaxy and from its halo, as is often assumed in these models, or because the conversion of gas into stars is slowed in low mass systems.

We now derive the scaling between the stellar mass of a disk galaxy and the mass of its dark matter halo from the *slope* of the $\mu_* - M_*$ relation. If we adopt the assumptions of the simple model, we can write

$$\mu_* \propto M_*/R_d^2 \propto \epsilon M_{halo}/R_{halo}^2 \propto \epsilon M_{halo}^{1/3} \propto \epsilon^{2/3} M_*^{1/3}, \qquad (4)$$

where $\epsilon \propto M_*/M_{halo}$ is the efficiency with which the disk has converted the available gas into stars. The Fall & Efstathiou arguments are only directly relevant to the formation of disk galaxies, while the conditional density distributions shown in Fig. 7 are derived using all galaxies in the sample. At stellar masses greater than $10^{10} M_\odot$, a large fraction of the galaxies are bulge-dominated systems. In order to clarify the scaling properties of our two principal classes of galaxy, we define two subsamples which eliminate most of the mixed systems: i) a sample of late-type galaxies with $C < 2.6$ and $D_n(4000) < 1.55$ (27200 galaxies); and ii) a sample of early-type galaxies with $C > 2.6$ and $D_n(4000) > 1.55$ (34661 galaxies). Fig. 11 demonstrates that these cuts divide young, disk-dominated systems from old, bulge-dominated systems surprisingly cleanly.

The $\mu_* - M_*$ relation of our late-type subsample is shown in the left panel of Fig. 14, while the right panel shows the corresponding relation for early-types. It is striking that the $\mu_* - M_*$ relation for each subsample can be described by a single power-law, but that the slope is very different in the two cases. (Note that there are few late-type galaxies with stellar masses above $2 \times 10^{11} M_\odot$ and few early-types with M_* below $10^{10} M_\odot$.) Fig. 14 also shows that early-type galaxies of given stellar mass have higher stellar surface densities than late-type galaxies of the same mass. This difference is largest for the lowest mass objects and disappears for the most massive systems in our samples.

Fitting to the dominant part of the population of late-type galaxies (i.e. over the stellar mass range $10^8 - 3 \times 10^{10} M_\odot$) , we find $\mu_* \propto M_*^{0.6}$, so that $\epsilon \propto M_*^{0.4} \propto M_{halo}^{2/3}$ and $R_d \propto M_*^{0.2}$. The star formation efficiency for disk galaxies apparently increases with mass much as predicted by simple feedback models. For low mass systems Tremonti et al (2002) find the gas phase metallicity to increase with stellar mass as $Z \propto M_*^{0.5}$, suggesting a similar dependence of overall star formation efficiency on stellar mass.

For early-type galaxies, we fit over the range $3 \times 10^{10} - 10^{12} M_\odot$ and obtain $\mu_* \propto M_*^{0.2}$, which implies that $R \propto M_*^{0.4}$. For constant ϵ equation (4) predicts a very similar scaling, $R \propto M_*^{0.33}$. A possible interpretation is thus that the star formation efficiency in these galaxies depends little on stellar mass, and that their size is approximately proportional to that of the dark halos in which they formed. Their metallicities would then also be expected to show little mass dependence, as is indeed the case for *star-forming* galaxies of similar stellar mass (Tremonti et al 2002). A simple explanation for the saturation of star formation efficiency would then be that it approaches unity in these systems, and that the corresponding star formation rates are so high that gas is almost all converted into stars before the systems can approach equilibrium and form a disk.

It seems likely that the assembly of bulge-dominated galaxies involved chaotic processes such as mergers or inhomogenous, rapidly star-forming collapse, which, for most systems, must have completed well before the present day. The halo sizes and surface densities relevant for early-type galaxies are thus likely to be defined at higher effective redshift than those relevant for late-type galaxies, even at similar stellar mass. This may explain why early-type galaxies in Figure 14 have higher surface densities than late-type galaxies of similar mass. The scatter in surface density (and size) is also smaller for early-type than for late-type galaxies, as is very evident in Figure 14 as well as in Figures 7 and 8. In a merger picture this smaller scatter could be a consequence of averaging over the mass–size distribution of several significant progenitors.

We note that the Lyman Break Galaxies (LBGs) at high redshift can plausibly be identified with these progenitors. Pettini et al.(2001) have derived a mean effective dynamical mass of $1.3 \times 10^{10} M_{\odot}$ within a mean half-light radius of 2.3 kpc for a sample of LBGs at $z \sim 3$. Shapley et al.(2001) and Papovich et al. (2001) have estimated the stellar massses of LBGs using their observed rest-frame ultraviolet and optical spectral energy distributions. These agree well with the dynamical mass estimates. Lyman Break Galaxies thus have characteristic surface mass densities of $\sim 10^9 M_{\odot}$ kpc^{-2}, quite similar to those of present-day early-type galaxies. Moreover, if the star-formation associated with the Lyman Break Galaxies is integrated from from $z \sim 2$ to 6, one finds that they could have produced a significant fraction of the stellar mass in early-type galaxies today (Steidel et al. 1999; Thompson et al 2001).

We have argued that the star formation histories of galaxies depend primarily on their stellar surface mass densities, rather than on their stellar masses. Figs. 12 and 13 show that at fixed surface mass density, the fraction of galaxies that have experienced recent bursts is nearly independent of stellar mass. Likewise Fig. 14 demonstrates that at given mass, 'young' disk-dominated galaxies have lower surface mass densities than 'old' bulge-dominated galaxies. Unfortunately, we are missing important information about the gas content of our galaxies. It is likely that the galaxies with low stellar surface mass densities have high gas fractions. Indeed, it has been shown by McGaugh & De Blok (1997) that the gas fractions of spiral galaxies are strongly correlated both with their luminosities and with their surface brightnesses. Kennicutt (1983;1998b) has shown that the star formation rates in disk galaxies are strongly correlated with their gas surface densities. Thus the trend of younger stellar ages with lower *stellar* surface densities may simply reflect an increase in star formation rate at high gas surface density. Moreover, as argued by Sakamoto et al (1998), disk galaxies with high gas-to-total mass ratios are more unstable than disk galaxies with low gas-to-total mass ratios. Disk instabilities may thus be responsible for the burst-dominated mode of star formation in low stellar surface density, gas-rich systems. High stellar surface density galaxies, on the other hand, are gas-poor. Any bursts occurring in these obejcts will involve only a small fraction of their total stellar mass and will most often be undetectable with our methods.

In the framework of hierarchical models of galaxy formation, the trend of younger mean stellar ages with decreasing stellar mass is puzzling at first sight, since most low mass dark matter halos formed at early epochs. If all the gas cooled off and formed stars when these halos were assembled, low mass galaxies would all have very old stellar populations (Kauffmann, White & Guiderdoni 1993). However, we have seen that non-gravitational processes such as supernova feedback may play an important role in regulating the rate at which stars form in these systems. To explain the observations, these processes must slow the conversion of gas into stars so that low mass systems remain gas rich at the present day and have low overall efficiencies for turning gas into stars.

Conversely, it may appear puzzling that star formation has terminated in the majority of high mass galaxies, because the hierarchical model claims that these systems were assembled relatively late. As noted above, several lines of argument suggest that star formation was both efficient and rapid in the progenitors of these systems, so that the final stages of their assembly may have involved rather little dissipation or star formation. In current models, galaxies that fall into groups and clusters are stripped of their reservoir of gas. As a result, their star formation rates decline and their colours redden (see for example Diaferio et al 2001). This is unlikely to explain why the *majority* of massive galaxies do not form stars at the present day, because many of these objects do not reside in rich groups and clusters. In such systems, gas must somehow be prevented from cooling and forming stars after their bulge has formed.

Finally, it will be important to understand the physical origin of the characteristic mass scale that is so strikingly imprinted on the galaxy population. The structural properties and formation paths of dark matter halos vary smoothly with mass. The abrupt transition in the stellar ages, star formation histories and structure of galaxies that we find at $3 \times 10^{10} M_\odot$ can only be explained by star formation and/or supernova feedback processes. We believe that this tension between the predictions of simplified phenomenological models of galaxy evolution and the trends seen in the data will lead to new insight into the physical processes that regulate how galaxies form and evolve. We intend to address these issues in more detail in future work.

We thank David Weinberg and Eric Bell for helpful discussions and comments. S.C. thanks the Alexander von Humboldt Foundation, the Federal Ministry of Education and Research, and the Programme for Investment in the Future (ZIP) of the German Government for their support.

The Sloan Digital Sky Survey (SDSS) is a joint project of The University of Chicago, Fermilab, the Institute for Advanced Study, the Japan Participation Group, The Johns Hopkins University, Los Alamos National Laboratory, the Max-Planck-Institute for Astronomy (MPIA), the Max-Planck-Institute for Astrophysics (MPA), New Mexico State University, Princeton University, the United States Naval Observatory, and the University of Washington. Apache Point Observatory, site of the SDSS telescopes, is operated by the Astrophysical Research Consortium (ARC).

Funding for the project has been provided by the Alfred P. Sloan Foundation, the SDSS member institutions, the National Aeronautics and Space Administration, the National Science Foundation, the U.S. Department of Energy, the Japanese Monbukagakusho, and the Max Planck Society. The SDSS Web site is http://www.sdss.org/.

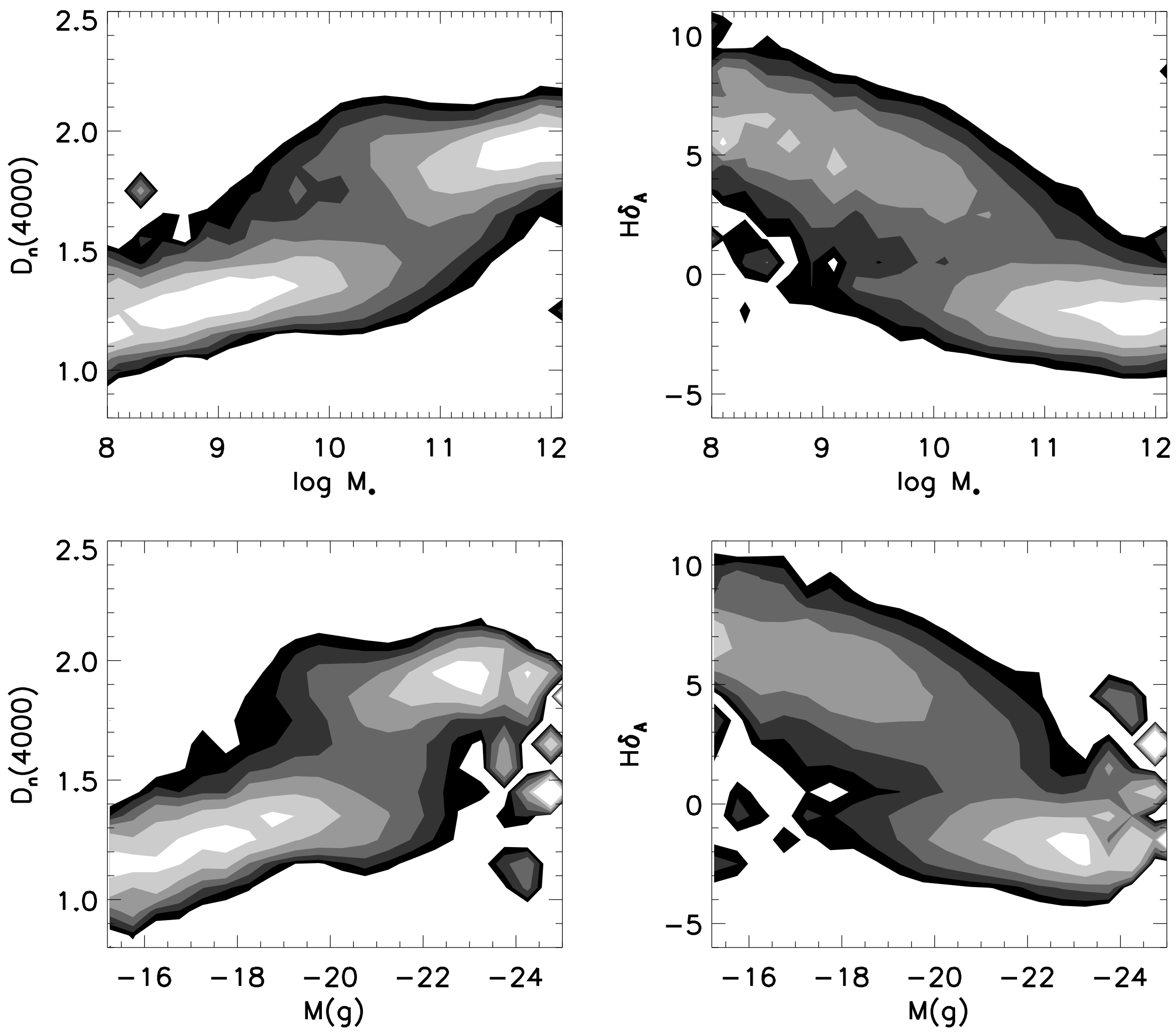

Figure 1: Conditional density distributions showing trends in the stellar age indicators $D_n(4000)$ and $H\delta_A$ as functions of the logarithm of stellar mass and of g-band absolute magnitude. Galaxies have been weighted by $1/V_{max}$ and the bivariate distribution function has been normalized to a fixed number of galaxies in each bin of $\log M_*$ or M(g). Here and in all subsequent contour plots, each contour represents a factor two change in density.

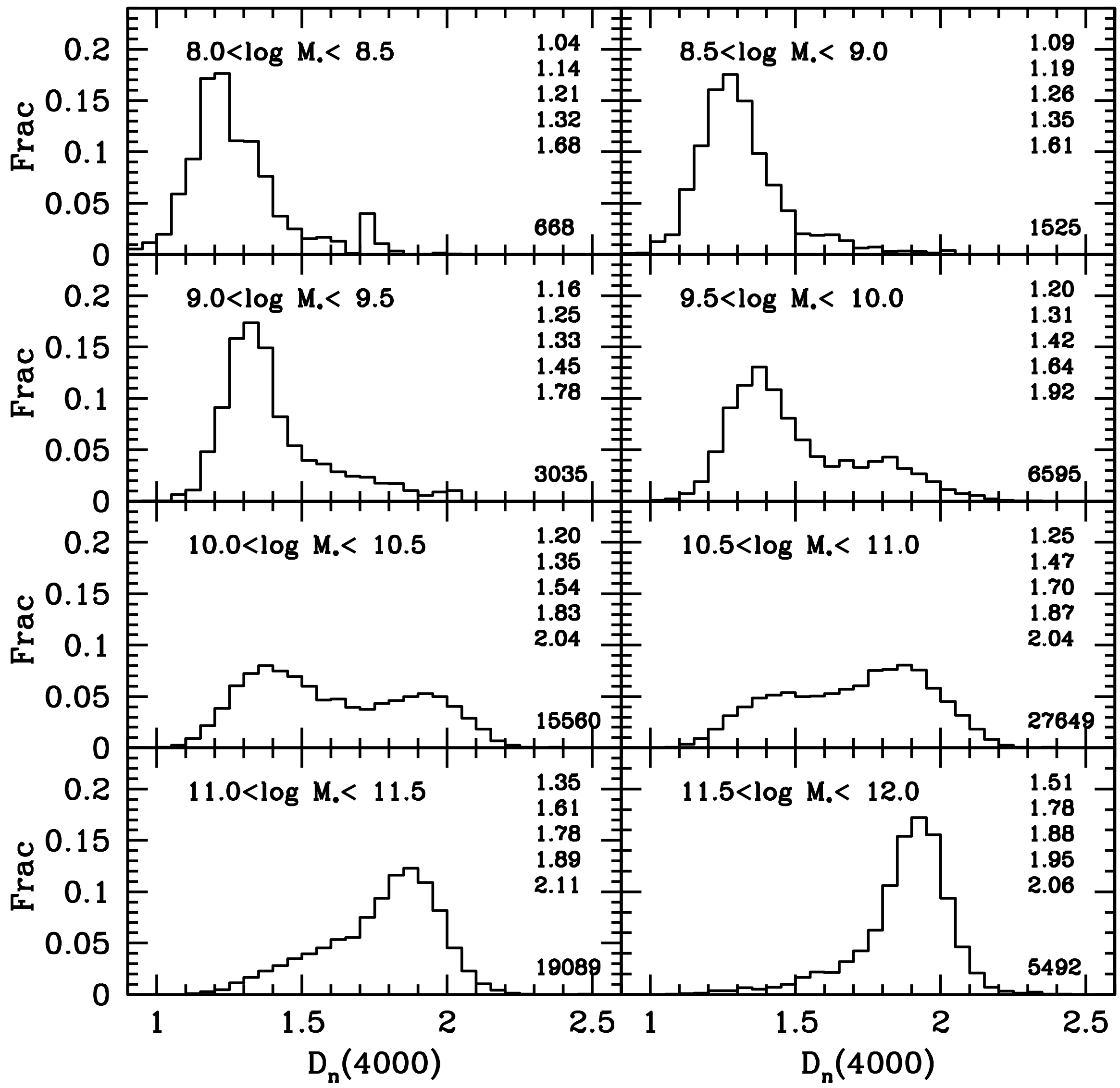

Figure 2: Histograms showing the fraction of galaxies as a function of $D_n(4000)$ in 8 different ranges of stellar mass. The numbers in the upper right corner of each panel list, from top to bottom, the 5th, 25th, 50th, 75th and 95th percentiles of the distribution. The number in the lower right corner is the number of galaxies contributing to the histogram.

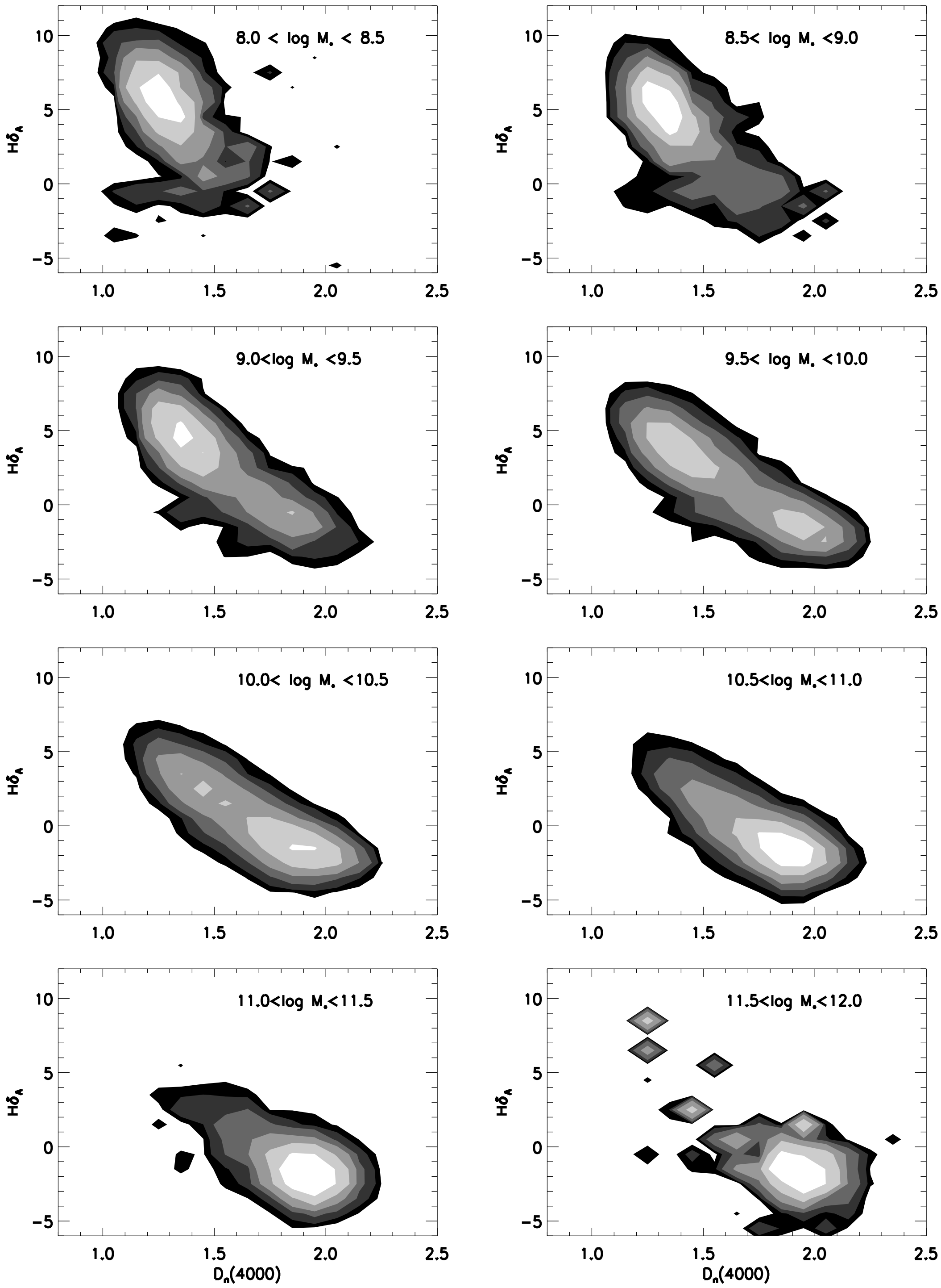

Figure 3: The bivariate distribution function of $H\delta_A$ and $D_n(4000)$ in 8 ranges of stellar mass.

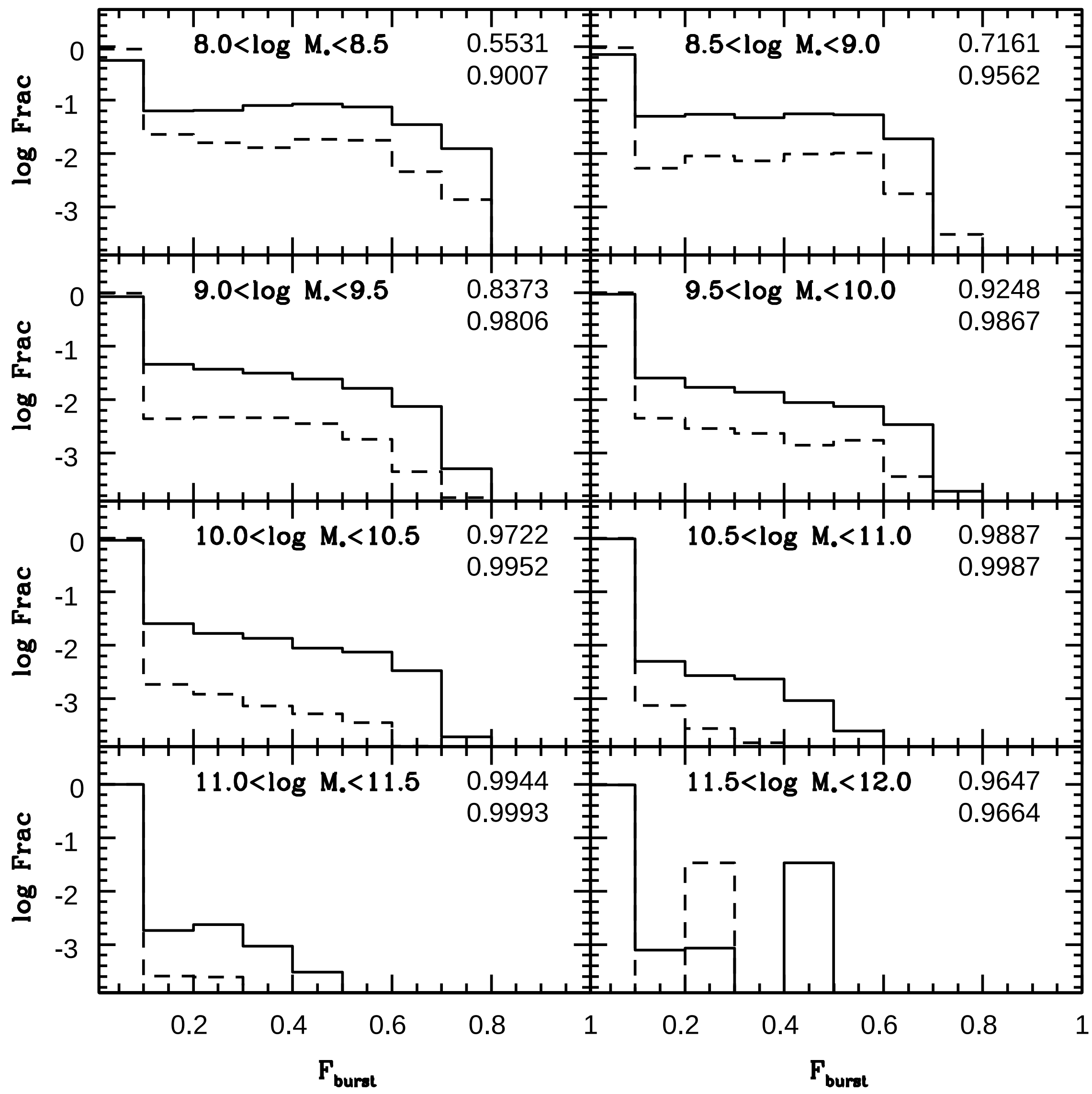

Figure 4: The solid histograms show the distributions of galaxies as a function of median value of the likelihood distribution of F_{burst} in 8 stellar mass ranges. The dashed histograms show distributions of galaxies as a function of the lower 2.5 percentile of the likelihood distribution of F_{burst}. The numbers on each panel indicate the fraction of galaxies in each mass bin with zero values of the median (upper) and the 2.5 percentile point (lower).

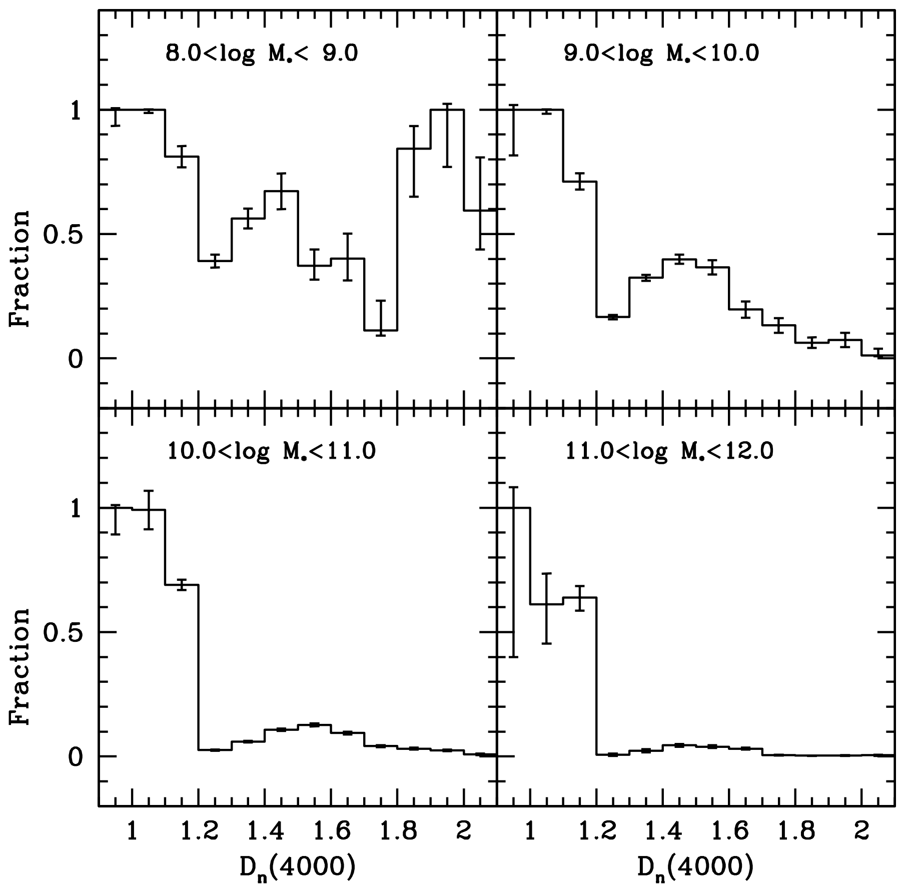

Figure 5: The fraction of galaxies with $\bar{F}_{burst} > 0$ is plotted as a function of $D_n(4000)$ for 4 stellar mass ranges. Error bars ($\pm$ 68% confidence) based on the number of galaxies contributing to each bin are indicated.

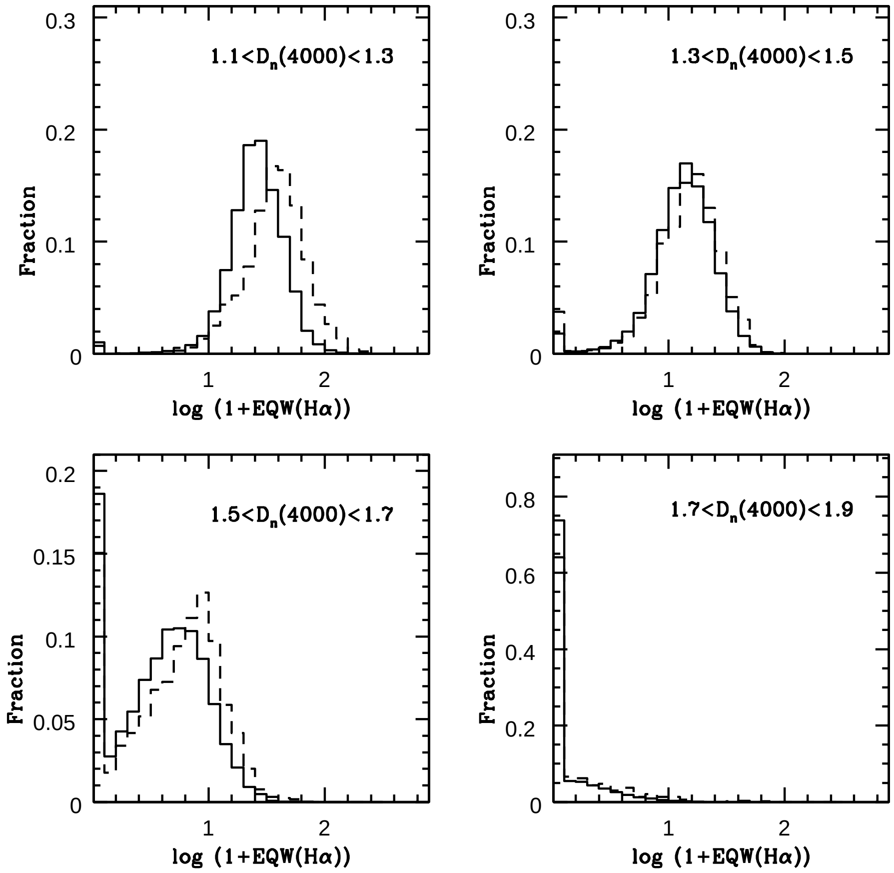

Figure 6: The distribution of Hα equivalent widths for galaxies with $\bar{F}_{burst} > 0$ (dashed)) is compared to that for galaxies with $\bar{F}_{burst} = 0$ (solid) for four different ranges in the value of the D$_n$(4000) index.

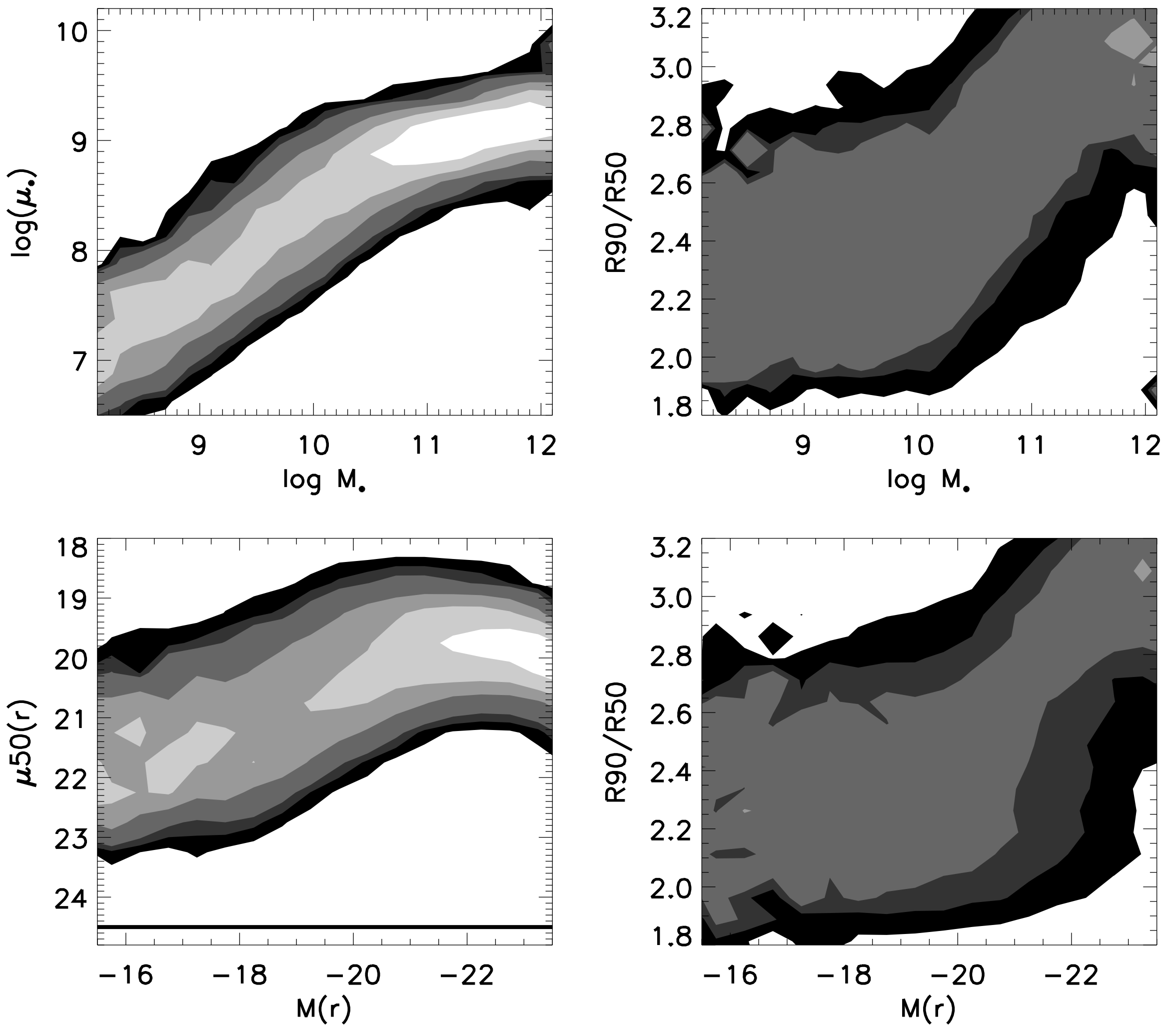

Figure 7: Conditional density distributions showing trends in the structural parameters μ_*, $\mu_{1/2}$ and $C = R90/R50$ as a function the logarithm of stellar mass and as a function of r-band absolute magnitude. Galaxies have been weighted by $1/V_{max}$ and the bivariate distribution function has been normalized to a fixed number of galaxies in each bin of $\log M_*$ and of r-band absolute magnitude. The line in the bottom left panel indicates the surface brightness completeness limit of the SDSS survey.

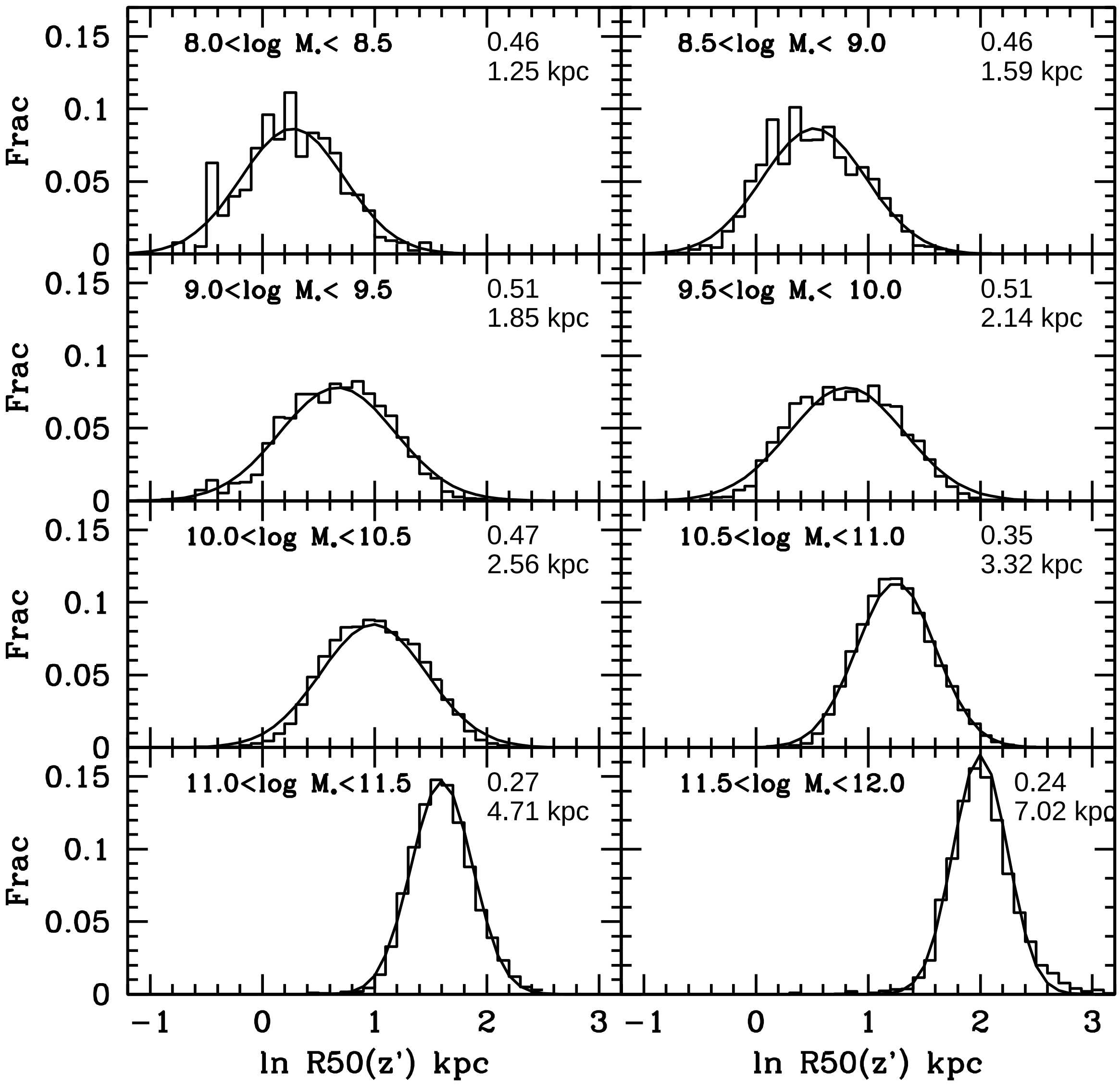

Figure 8: Histograms showing the fraction of galaxies as a function of the natural logarithm of the half-light radius in the z-band ($R50(z)$) in 8 different ranges of stellar mass. The curves show lognormal fits to the distribution and the numbers in each panel are the best-fit values of σ (top) and R_{med} (bottom).

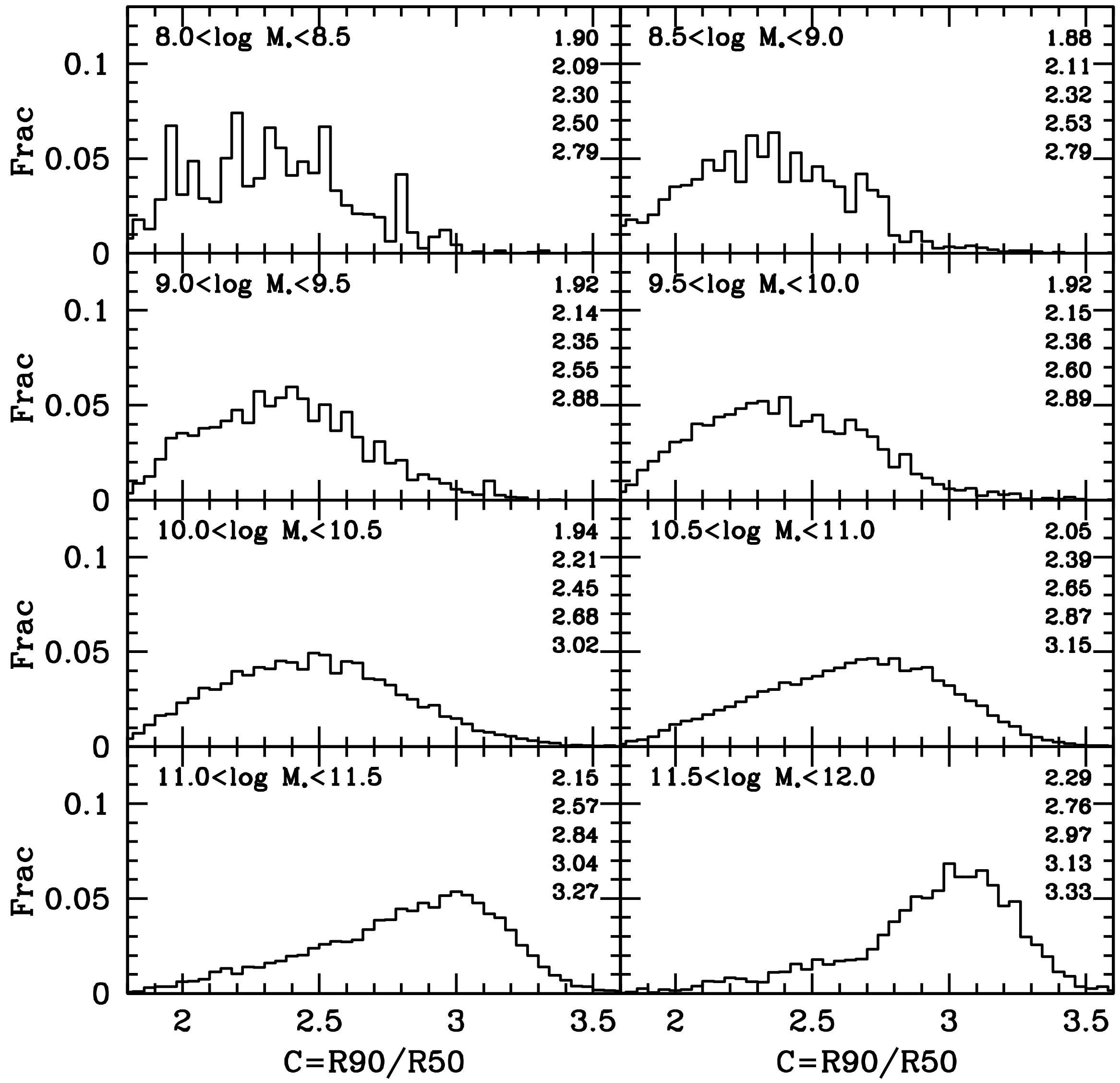

Figure 9: Histograms showing the distribution of galaxies as a function of C index for 8 different ranges of stellar mass. The numbers in each panel list, from top to bottom, the 5th, 25th, 50th, 75th and 95th percentiles of the distribution.

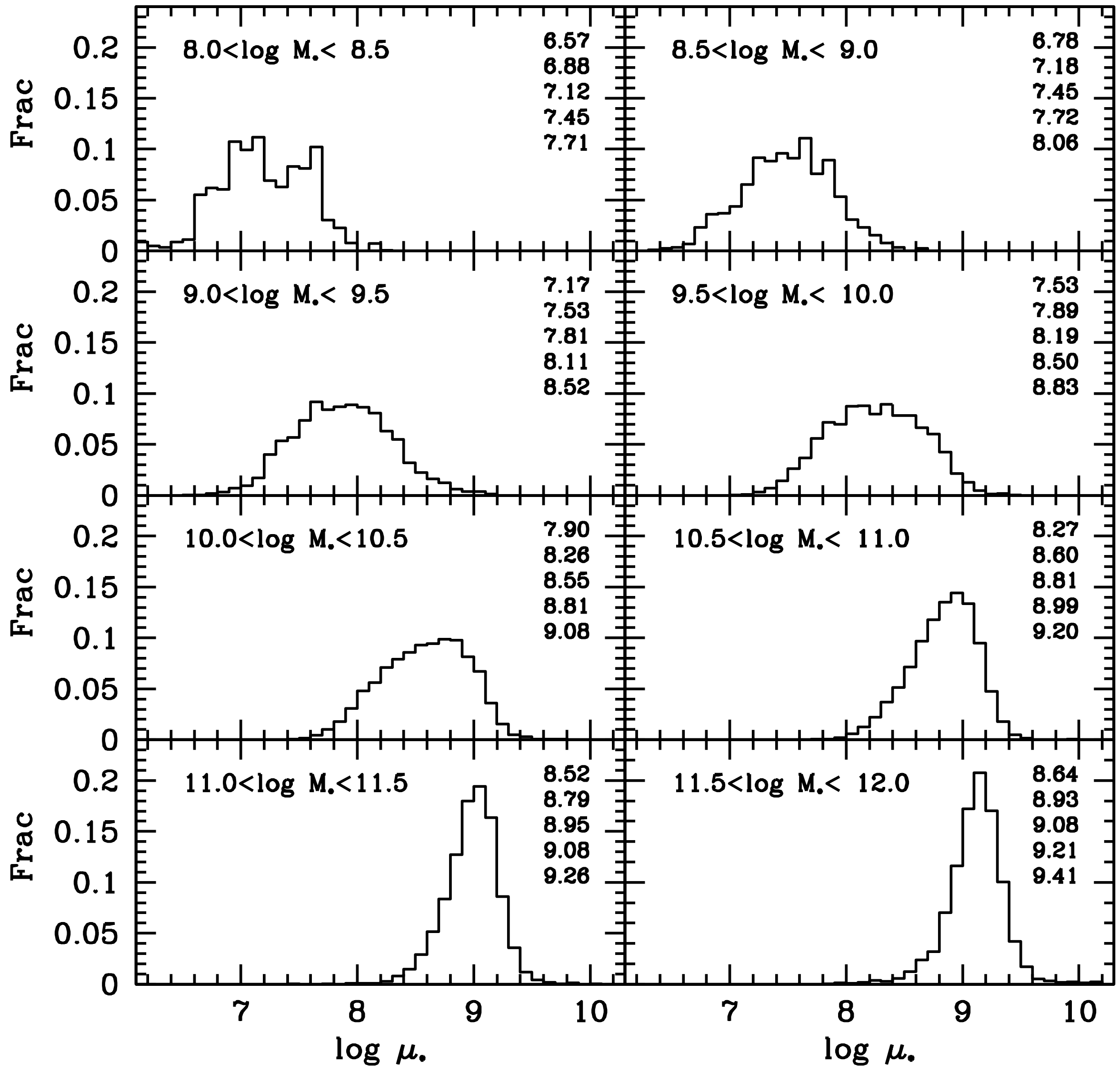

Figure 10: Histograms showing the distribution of galaxies as a function of $\log \mu_*$ for 8 different ranges in stellar mass. The numbers in each panel list, from top to bottom, the 5th, 25th, 50th, 75th and 95th percentiles of each distribution.

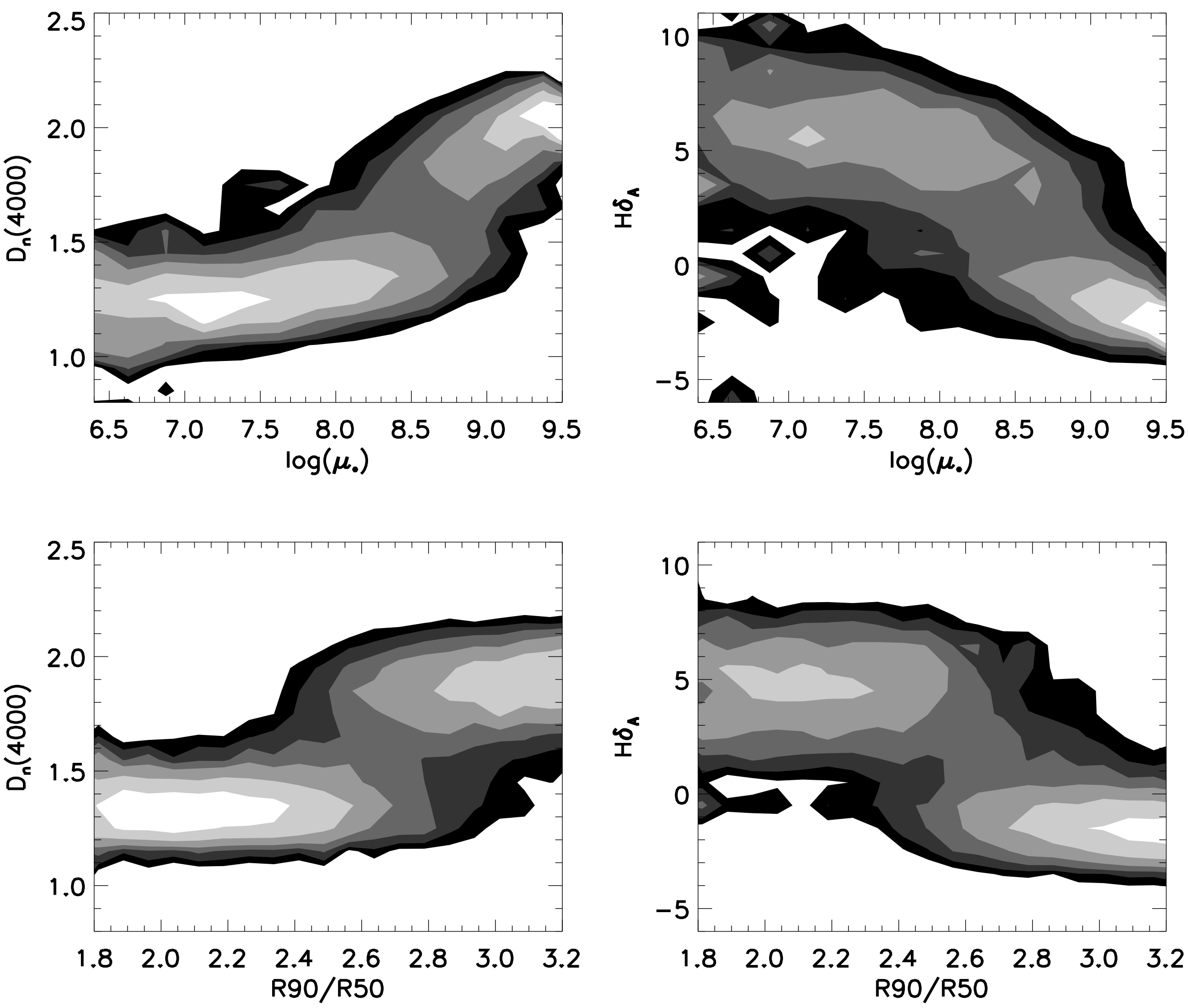

Figure 11: Conditional density distributions showing trends in the stellar age indicators $D_n(4000)$ and $H\delta_A$ as functions of the logarithm of the surface mass density μ_* and of the concentration index C.

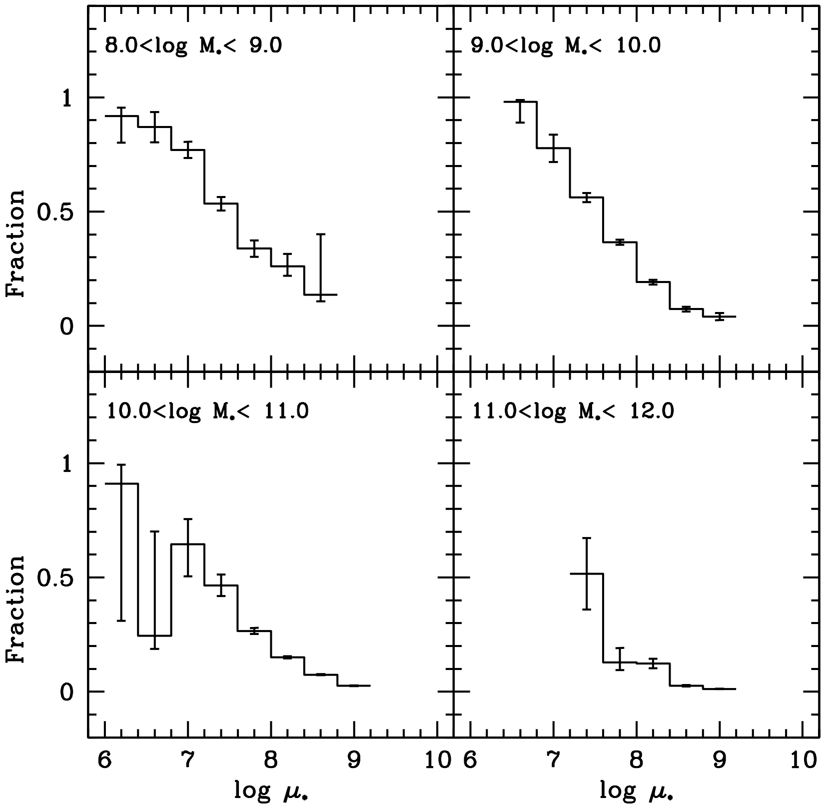

Figure 12: The fraction of galaxies with $\bar{F}_{burst} > 0$ is plotted as a function of $\log \mu_*$ for four stellar mass ranges. Error bars ($\pm$ 68% confidence limit) based on the number of galaxies contributing to each bin are indicated.

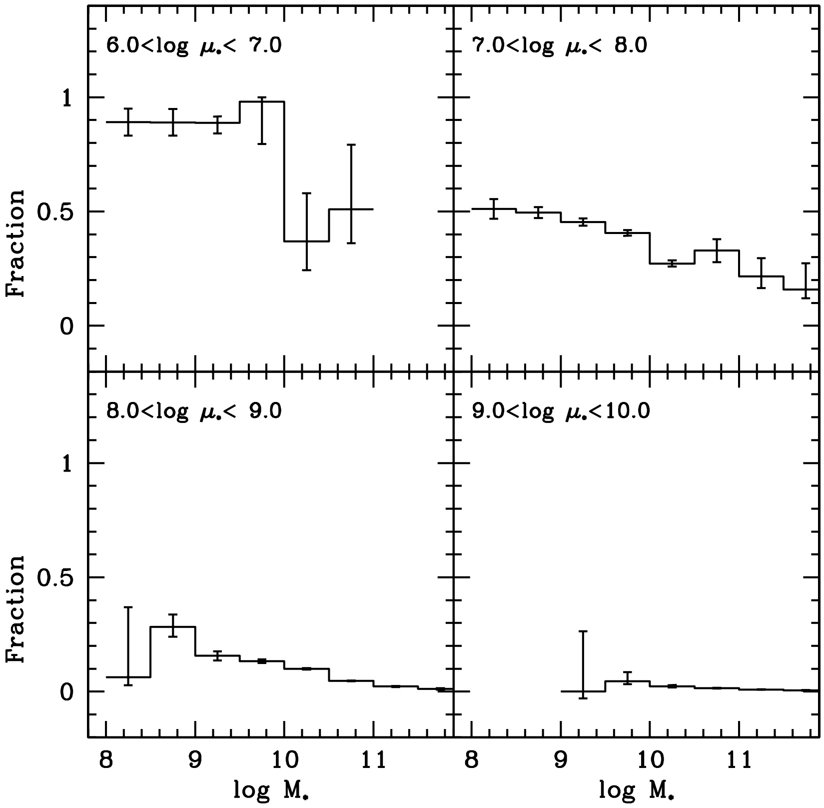

Figure 13: The fraction of galaxies with $\bar{F}_{burst} > 0$ is plotted as a function of $\log M_*$ for four disjoint ranges of $\log \mu_*$.

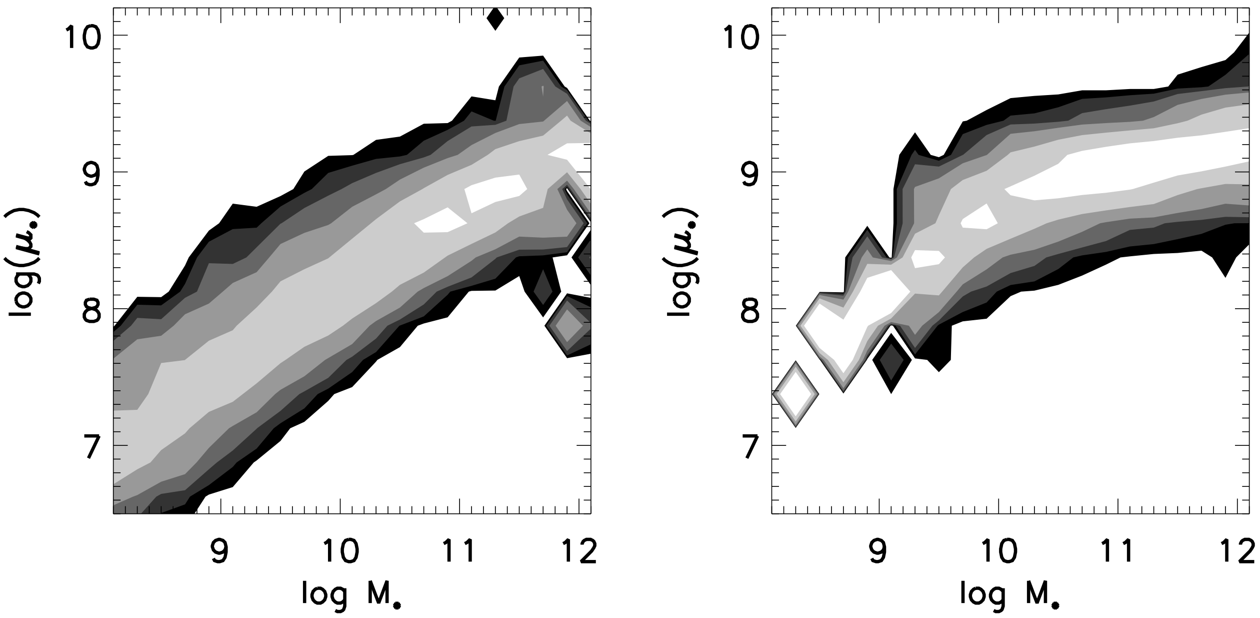

Figure 14: Conditional density distributions showing trends in μ_* as a function the logarithm of stellar mass for galaxies with $D_n(4000) < 1.55$ and $C < 2.6$ (left) and with $D_n(4000) > 1.55$ and $C > 2.6$(right).

References

Balogh, M.L., Morris, S.L., Yee, H.K.C., Carlberg, R.G., Ellingson, E., 1999, ApJ, 527, 54

Balogh, M.L., Christlein, D., Zabludoff, A.I., Zaritsky, D., 2001, ApJ, 557, 117

Barnes, J., Efstathiou, G., 1987, ApJ, 319, 575

Bell, E.F., de Jong, R.S., 2001, ApJ, 550, 212

Blanton, M.R., Dalcanton, J., Eisenstein, D., Loveday, J., Strauss, M.A., SubbaRao, M., Weinberg, D.H., Andersen, J.E. et al., 2001, AJ, 121, 2358

Boselli, A., Gavazzi, G., Donas, J., Scodeggio, M., 2001, AJ, 121, 753

Bruzual, A.G., Charlot, S., 1993, ApJ, 405, 538

Christlein, D., 2000, ApJ, 545, 145

Cole, S., Aragon-Salamanca, A., Frenk, C.S., Navarro, J.F., Zepf, S.E., 1994, MNRAS, 271, 781

Cole, S., Lacey, C., 1996, MNRAS, 281, 716

de Blok, W.J.G., van der Hulst, J.M., Bothun, G.D., 1995, MNRAS, 274, 235

de Blok, W.J.G., McGaugh, S.S., van der Hulst, J.M., 1996, MNRAS, 283, 18

Diaferio, A., Kauffmann, G., Balogh, M.L., White, S.D.M., Schade, D., Ellingson, E., 2001, MNRAS, 328, 726

Efstathiou, G., 2000, MNRAS, 317, 697

Fall, S.M., Efstathiou, G., 1980, MNRAS, 193, 189

Fukugita, M., Ichikawa, T., Gunn, J.E., Doi, M., Shimasaku, K., Schneider, D.P., 1996, AJ, 111, 1748

Grebel, E.K., 2000, Proc. 33rd ESLAB Symposium, ESA SP-445, eds.F.Favata, A.A.Kaas & Wilson (Noordwijk:ESA), 87-98 (astro-ph/0005296)

Gunn, J.E., Carr, M., Rockosi, C., Sekiguchi, M., Berry, K., Elms, B., de Haas, E., Ivezic, Z. et al, 1998, AJ, 116, 3040

Hogg, D.W., Finkbeiner, D.P., Schlegel, D.J., Gunn, J.E., 2001, AJ, 122, 2129

Hubble, E.P., 1926, ApJ, 64, 321

Kauffmann, G., White, S.D.M., Guiderdoni, B., 1993, MNRAS, 264, 201

Kauffmann, G., Heckman, T.M., White, S.D.M., Charlot, S., Tremonti, C., Peng, E.W., Seibert, M., Bernardi, M. et al. 2002, MNRAS, submitted (Paper I)

Kennicutt, R.C., 1983, ApJ, 272, 54

Kennicutt, R.C., 1998a, ARA&A, 36, 189

Kennicutt, R.C., 1998b, ApJ, 498, 541

Kroupa, P., 2001, MNRAS, 322, 231

Kuntschner, H., Lucey, J.R., Smith, R.J., Hudson, M.J., Davies, R.L., 2001, MNRAS, 323, 615

Lemson, G., Kauffmann, G., 1999, MNRAS, 302, 111

Lin, H., Kirshner, R.P., Shectman, S.A., Landy, S.D., Oemler, A., Tucker, D.L., Schechter, P.L., 1996, ApJ, 464, 60

Loveday, J., Peterson, B.A., Efstathiou, G., Maddox, S.J., 1992, ApJ, 390,338

Marzke, R.O., Geller, M.J., Huchra, J.P., Corwin, H.G., 1994, AJ, 108, 437

Marzke, R.O., Da Costa, L.N., Pellegrini, P.S., Willmer, C.N.A., Geller, M.J., 1998, ApJ, 503,617

McGaugh, S.S., de Blok, W.J.G., 1997, ApJ, 481, 689

McKee, C.F., Ostriker, J.P., 1977, ApJ, 218, 148

Mo, H.J., Mao, S., White, S.D.M., 1998, MNRAS, 295, 319

Papovich, C., Dickinson, M., Ferguson, H.C., 2001. ApJ, 559, 620

Pettini, M., Shapley, A.E., Steidel, C.C., Cuby, J.G., Dickinson, M., Moorwood, A.F.M., Adelberger, K.L., Giavalisco., M., 2001, ApJ, 554, 981

Pier, J.R. et al., 2002, AJ, submitted

Roberts, M.S. & Haynes, M.P., 1994, ARA&A, 32, 115

Sakamoto, K., Okumura, S.K., Ishizuki, S., Scoville, N., 1999, ApJ, 525, 691

Shapley, A.E., Steidel, C.C., Adelberger, K.L., Dickinson, M., Giavalisco., M., Pettini, M., 2001, ApJ, 562, 95

Shimasaku, K., Fukugita, M., Doi, M., Hamabe, M., Ichikawa, T., Okamura, S., Sekiguchi, M., Yasuda, N. et al, 2001, AJ, 122, 1238

Smith, J.A., Tucker, D.L., Kent, S., Richmond, M.W., Fukugita, M., Ichikawa, T., Ichikawa, S.I.,Jorgensen, A.M. et al. 2002, AJ, in press

Steidel, C.C., Adelberger, K.L., Giavalisco, M., Dicksinson, M., Pettini, M., 1999, ApJ, 519, 1

Stoughton, C., Lupton, R.H., Bernardi, M., Blanton, M.R., Burles, S., Castander, F.J., Connolly, A.J., Eisenstein, D.J. et al., 2002, AJ, 123, 485

Strauss, M.A., Weinberg, D.H., Lupton, R.H., Narayanan, V.K., Annis, J., Bernardi, M., Blanton, M., Burles, S. et al, 2002, AJ, submitted

Strateva, I., Ivezic, Z., Knapp, G.R., Narayanan, V.K., Strauss, M.A., Gunn, J.E., Lupton, R.H., Schelger, D. et al, 2001, AJ, 122, 1861

Thompson, R.I., Weymann, R.J., Storrie-Lombardi, L.J., 2001, ApJ, 546, 694

Trager, S.C., Worthey, G., Faber, S.M., Burstein, D., Gonzalez, J.J., 1998, ApJS, 116, 1

Tremonti, C.A. et al., 2002, in preparation

Warren, M.S., Quinn, P.J., Salmon, J.K., Zurek, W.H., 1992, ApJ, 399, 405

White, S.D.M., Frenk, C.S., 1991, ApJ, 379, 52

Worthey, G., Ottaviani, D.L., 1997, ApJS, 111, 377

York D.G., Adelman J., Anderson J.E., Anderson S.F., Annis J., Bahcall N.A., Bakken J.A., Barkhouser R. et al., 2000, AJ, 120, 1579

Zucca, E., Zamorani, G., Vettolani, G., Cappi, A., Merighi, R., Mignoli, M., Stirpe, G.M., MacGillivray, H. et al., 1997, A&A, 326, 477